Detailed modelling of pixellated CdZnTe detectors for an accurate performance characterization of a multi-modality imaging system

Pedro Guerra *Graduate Student Member IEEE*, George Kontaxakis *Senior Member IEEE*, Dimitris Visvikis *Member IEEE*, Andres Santos *Senior Member IEEE* and Dimitra G. Darambara *Member IEEE*

Abstract– **Room temperature semiconductor detectors, such as CdZnTe (CZT), are promising candidates for the design and development of a true integrated multimodality imaging system. However, hitherto no detailed analysis of the real potential of such a CZT-based canner has been carried out. In this work we report the modifications and developments implemented to incorporate the first of its kind accurate modelling of pixellated CZT detectors in different configurations within the Geant4 application for tomographic emission (GATE) simulation platform. These models are required for an accurate simulation and a precise future analysis of the expected overall performance of the scanner. The quantitative assessment of the simulated data will result in an optimum pixellated CZT detector design with specifications that compensate transport properties in the crystal but also meet the requirements for an integrated PET/SPECT/CT multimodal system.**

I. INTRODUCTION

THE INTEREST in room temperature semiconductor detectors with high atomic numbers, like CdTe/CdZnTe, for gamma ray imaging has been steadily increased in the last decade, supported by recent advances in the crystal growth.

Monolithic CZT detectors are promising for medical applications and small animal imaging due to their high energy resolution within a wide range of energies that allows better scatter rejection and multi-isotope acquisition. The combination of large bandgap, excellent energy and spatial resolution, high stopping power and the capability of depth-of-interaction (DOI) measurement makes CZT the detector material of choice for the next generation of multimodality scanners for molecular imaging. Due to its properties, it seems feasible to piece together in a single detector module positron and single photon emission (PET/SPECT) and x-ray computer tomography (CT) as well as to integrate it within a magnet.

Most studies up to now focus on the investigation of the properties of a single detector; however the full potential of a CdZnTe based scanner remains still under consideration [1], mostly due to an incomplete modelling of the CZT detector.

Such performance analyses are based on simulation tools that include detailed models of the underlying physics and scanner characteristics. Among these tools, the Geant4 application for tomographic emission (GATE) [2] has recently become very popular due to its flexibility to model various existing scanners and the accuracy of its simulations compared to experimental data. Nevertheless, GATE current models focus mostly on scintillator-based detectors and the accurate modelling of the CZT is rather limited.

A number of publications have dealt in the past with the modeling of charge transport in semiconductor detectors. Early works assumed an uniform electric field, while later works tend to consider more complicated electric field profiles, where numerical techniques become unavoidable [3-6]. For example, the 3D model presented by *Mathy et al* involves the finite element transient computation of the adjoint transport equation, a Monte Carlo simulation of the photon transport and the electronic signal processing including an accurate noise model [7].
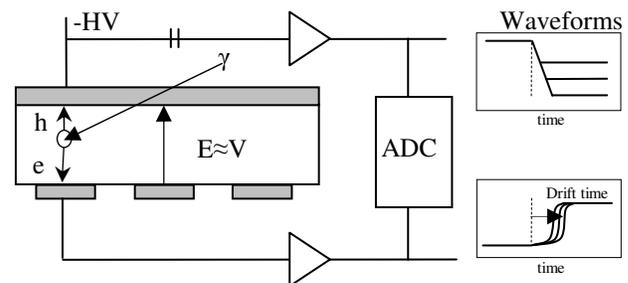
Figure 1: Basic diagram of a pixellated CZT detector with biasing voltage V and width d. The waveform of the expected signals at the anode and cathode are shown on the right.

The aim of this work is to develop a computationally simple model of the pixellated CZT detector and implement the required digitizer modules as well as the necessary modifications of the GATE source code in order to improve the GATE simulations of CZT pixellated detectors in different configurations with simultaneous cathode and anode pixel readout.

II. DETECTOR MODEL

The proposed multimodality scanner consists of several detector modules, each one comprising one or more CZT slabs. The interaction of a gamma-ray with the semiconductor material causes the excited electrons to jump to higher energy bands creating an excess of charge; under the presence of an electric field both electrons and holes are driven towards the anode and cathode electrodes respectively, inducing a voltage signal, as shown in Figure 1, that provides information about the deposited energy measurement and the position of interaction.

Unlike a scintillator crystal, in a semiconductor detector there is a significant dependence of the induced charge on the interaction point within the slab. Single polarity charge sensing through a coplanar grid anode has been widely applied to overcome the poor hole transport; however cathode sensing is usually required to resolve the depth of interaction and the timing of the event. In such a detector configuration, the signal on the anode is close to depth independent while the cathode signal varies approximately linearly with the distance. These and other effects are very well explained by the Schockley-Ramo theorem [8].

The usual model for charge collection in semiconductors consists of the continuity equation for excess charge carrier's densities. The charge induced at a selected electrode k by the drift of the electron density $n(x,t)$, during the time interval t', is calculated using Ramo's formulation as [6]:

$$\Delta Q_k = \int_0^{t'} dt \int_\Omega n \cdot \mu_n \cdot \nabla \psi \cdot \nabla \varphi_k \, d\Omega \tag{1}$$

Where $\psi(x)$ is the operating potential, $\varphi(x)$ is the weighting potential and μ_n is the electron mobility potential. In order to be able to incorporate Ramo's theorem into GATE at a reasonable computational cost several simplifications are required A feasible solution consists on assuming a 1-D version of the theorem [9] and combining it with charge recombination. In this case, the charge induced by a gamma-ray deposition at x_o that creates N_o electrons with mobility μ_e and life time τ_e travelling along the path towards the anode is approximated by:

$$\Delta Q_k = q \cdot N_0 \cdot \int_L e^{-(x-x_0)/\lambda_e} \cdot \varphi'_0(x) \cdot dx$$
$$\lambda_e = (\mu_e \cdot \tau_e) \cdot E = (\mu_e \cdot \tau_e) \cdot V/d \tag{1}$$

Where V is the biasing voltage and d is the detector's thickness.

The value of the weighting potential φ_k is mainly a function of the material properties and the detector geometry, and it can be computed in detail using finite element methods (FEM), as shown in Figure 2. As an example, if the semiconductor detector consisted on two parallel readout plates, one at the anode and one at the cathode, the weighting potential could be approximated by $\varphi(x)=x/d$ and further development of (1) would lead to the Hetch equation for the electrons.

$$\Delta Q_k = N_0 \cdot \frac{\lambda_e \cdot q}{d} \cdot \left(1 - e^{-\frac{d}{\lambda_e}}\right) \tag{2}$$
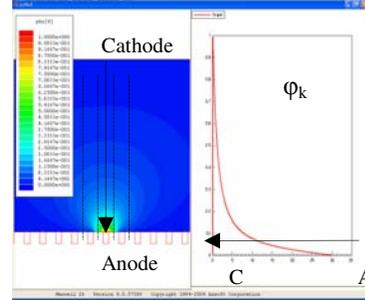
Figure 2: FEM simulation for φ_0 computation with a 32 mm thick CZT slab (left). Weighting function along the line between the anode and cathode (right).

In order to efficiently compute the induced charge ΔQ for a given energy deposition $N_o q$ at location x_o a closed form of (1) is preferred. The simplest solution approximates the weighting function $\varphi(x)$ with an exponential function with a decay constant τ that satisfies boundary conditions at the anode and cathode, as it is shown in (4).

$$\varphi(x) \approx \frac{e^{-d/\tau}}{1-e^{-d/\tau}} \cdot \left(e^{x/\tau} - 1\right)$$
$$\varphi'(x) \approx \frac{e^{-d/\tau}}{1-e^{-d/\tau}} \cdot \frac{1}{\tau} \cdot e^{x/\tau} \tag{3}$$
$$\varphi(0) = 0 \quad \varphi(d) = 1$$

Assuming the previous approximation, it is shown that the induced charge ΔQ is given by the following expression:

$$\Delta Q_k = \frac{\lambda_e^* \cdot N_0 \cdot q}{\tau} \cdot \frac{e^{\frac{x_0-d}{\lambda_e}}}{1-e^{-d/\tau}} \cdot \left(1 - e^{\frac{x_0-d}{\lambda_e^*}}\right) \tag{4}$$
$$\lambda_e^* = \frac{\lambda_e \cdot \tau}{\lambda_e - \tau}$$
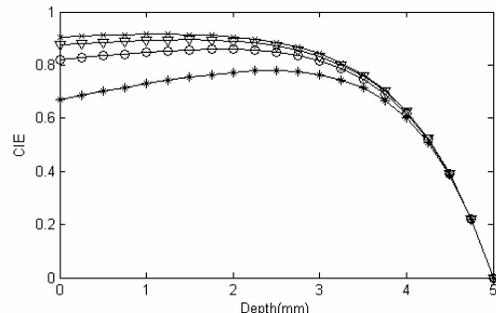
Figure 3: Calculated CIE for $\mu\tau_e=1(*)$, 2(o), 3(∇) and $4\times10^{-3}(x)$ cm^2/V without noise and 500V bias, with $\mu\tau_e \gg \mu\tau_h$.

$$CIE = \frac{\lambda_e^*}{\tau} \cdot \frac{e^{\frac{x_0-d}{\lambda_e}}}{1-e^{-d/\tau}} \cdot \left(1 - e^{\frac{x_0-d}{\lambda_e^*}}\right) \qquad (5)$$

The detector charge induction efficiency (CIE) is computed as the ratio between the deposited energy and the readout energy, which is depth dependant due to electron trapping. The model-based CIE, shown in , has been computed for different electron transport properties, with a profile that very well agrees with the solution of the drift-diffusion equation presented in [10].

The simplified model shown in (5) is extended to take into account interpixel charge sharing and crosstalk. In order to estimate the shared charge, we will assume that the energy deposition at x_o generates an electron cloud of finite size which, as a first approximation, is modeled as a cube of side D. The implemented simulation model computes the proportion of the cube that is contained at each pixel and creates a new GATE pulse at each of the affected detector pixels. Charge sharing will be mostly noticed in areas near the edges, where a fraction of this charge will belong to a pixel and another fraction to a neighboring pixel, as it is shown in Figure 4.
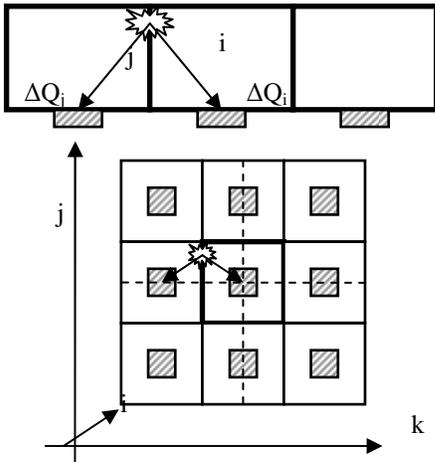
Figure 4: Charge sharing diagram. A cloud of electrons is generated, which may drift to different pixels.
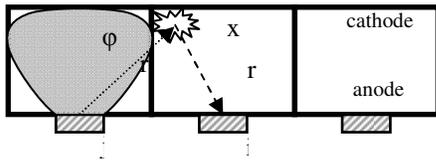
Figure 5: Crosstalk diagram. Pixel weighting potential extends beyond pixels limits inducing crosstalk.

Crosstalk refers to charge induction at anode j caused by charges that are collected by anode i, as it is shown in Figure 5. According to the Ramo's theorem, crosstalkI is explained by a weighting function whose volume of sensitivity is bigger that the pixel itself, situation that is shown in Figure 5, and it may be approximated as.

$$\Delta Q_j = -N_0 \cdot q \cdot \varphi_j(r_i) \qquad (6)$$

According to the previous equation, the explicit value of the weighting potential is needed, which in the implemented model is estimated based on the 3D analytical solution of the Laplace equation described in [11]. This solution assumes that the 3-D volume is contained between two infinite parallel planes representing the surfaces of the detector and the provided equations satisfy the original Dirichlet conditions of the two planes. Under the considered assumptions, the exact solution of the Laplace equation can be expressed as a series of elementary functions due to the reflected dipole layers equally spaced at *2kd*.

$$V = \sum_{k=-\infty}^{k=\infty} \varphi_0(x, y, z - 2kd) \qquad (7)$$

In the particular case where the pad is considered as rectangular, the solution reduces to:

$$\varphi_0(x, y, z) = \frac{1}{2\pi} \cdot \left(\begin{array}{l} \arctan \dfrac{(a-\xi)(b-\eta)}{z\sqrt{(a-\xi)^2 + (b-\eta)^2 + z^2}} + \ldots \\[2ex] \arctan \dfrac{(a-\xi)\eta}{z\sqrt{(a-\xi)^2 + \eta^2 + z^2}} + \ldots \\[2ex] \arctan \dfrac{\xi(b-\eta)}{z\sqrt{\xi^2 + (b-\eta)^2 + z^2}} + \ldots \\[2ex] \arctan \dfrac{\xi\eta}{z\sqrt{\xi^2 + \eta^2 + z^2}} \end{array} \right)$$

$$\xi = \frac{(x-x_1)(x_2-x_1) + (y-y_1)(y_2-y_1)}{a} \qquad (8)$$

$$\eta = \frac{-(x-x_1)(y_2-y_1) + (y-y_1)(x_2-x_1)}{b}$$

Where *a* and *b* are the readout pad's length and width respectively, (x_1, y_1) (x_2, y_2) (x_3, y_3) (x_4, y_4) are the *j* pad's corner coordinates in the user space and r_i:(x,y,z) is the interaction point x_o with respect to the anode *j*.
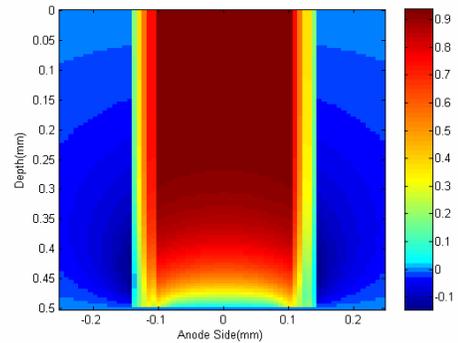
Figure 6: Calculated pixel CIE of the complete model for a 2x2x5 mm pixel at 500V bias with $\mu\tau_e = 3 \times 10^{-3}$cm^2/V and without noise

shows the estimated CIE when all the effects are included, which approximates very closely the numerical computations reported in [6].

III. GATE EXTENSIONS

GATE v2.2.0 has been extended to include the models previously presented. The original source code is extremely well structured and documented making it feasible to introduce custom modifications.

In particular, the *GatePulse* class has been extended to track energies at the anode and cathode. Additionally, a new digitizer module called *CZTEnergy* has been created in order to estimate the induced charges, which are modelled as an exponential function that combines the weighting function φ_0 with charge losses due to recombination as described in (5). Another module, called *CZTQsharing* has been implemented to model the collection of the electrons by different detector pixels.

Finally different modules, including *GateReadout* and *GateBlurring,* have been modified in order to account for the fact that two energies, anode and cathode, are being readout.

CZTQsharing	CZTEnergy	readout	Other
			digitizer
PadWidth	HoleLength0.625	EnableAnode	modules
	ElectronLength 62.5	EnableCathoa	
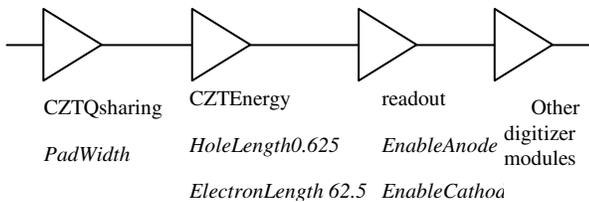
Figure 7: GATE's digitizer setup after extension for CZT modelling.

Simulations were run with for a gamma source consisting on a 2x5 cm plastic cylinder filled with [57]Co. A pixellated 5x10x10 mm CZT detector with 2x2 mm anode readout pads has been simulated
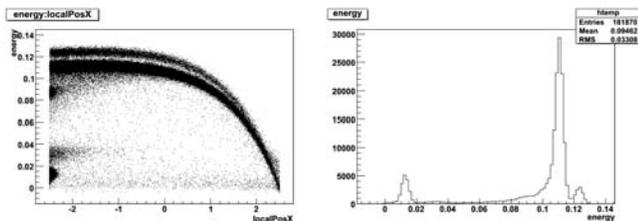
Figure 8: Simulated detected energy at the anode versus depth of interaction for a [57]Co source (left) and the resulting energy profile (right).

The simulated profile of the energy at the anode exhibits the characteristic tail on the low energy side of the spectrum, which is due to the abrupt fall of the induced charge for interactions close to the anode, as shown in Figure 7. Figure 8 presents the same data as seen by the cathode, where the weighting function can be considered as linear. Both plots match very well with the experimental data reported in [12]. Additionally the demonstration of the simulated cathode energy versus the anode energy, shown in Figure 9, matches the experimental biparametric data presented in [10].
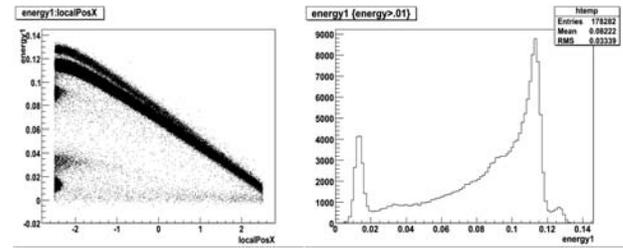
Figure 9: Simulated detected energy at the cathode versus depth of interaction for a [57]Co source (left) and the resulting energy profile (right)
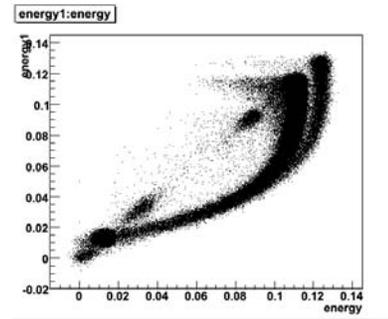
Figure 10: Cathode energy versus anode energy.

As previously stated the detector under consideration is intended for multimodality imaging. In the case of PET, the excellent spectrometric characteristics of pixellated CZT are somewhat limited by the long charge collection time of the material, which translate into a dependence of the timing signal with the depth of interaction. As a first approach, the timing resolution has been set to 15 ns FWHM to account for the drift time between the interaction point and the collecting anode of the 5 mm thick CZT slab, based on the experimental results reported in [13-15]..
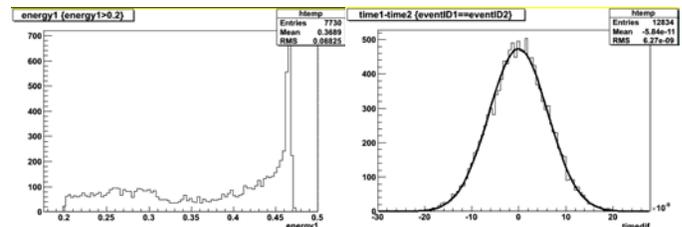
Figure 11: Energy spectra and timestamp difference distribution for 511 keV coincident events .

Simulations were also run for a positron source consisting on a 2x5 cm plastic cylinder filled with ^{18}F with the same 5x10x10 detector hereinbefore described. Figure 11 shows the estimated energy spectra and timing resolution at 511 keV obtained after the simulations.

IV. CONCLUSIONS AND ONGOING WORK

The GATE platform has been extensively validated against experimental data from numerous commercial scanners and has consolidated a design tool for the evaluation of new ideas and designs. However, existing systems focus primarily on scintillator-based detectors while semiconductor detectors, which are currently an interesting field of research for

multimodality molecular imaging, are not modelled with the same level of detail. A simplified model for pixellated semiconductor gamma ray detectors has been integrated into the GATE environment in order to cover this gap. The implemented models take into account the physics of the device's charge collection and enable system simulations for accurate performance characterization of a multimodality imaging system.

So far, simulation results match qualitatively experimental observations reported by different researchers and a further validation of the models is required based on FEM simulations and experimental data.

These simulation models will be the cornerstone of detailed simulations of the integrated multimodality system which will extend preliminary studies reported in [1], with the final aim of determining the optimum setup for a full scale multimodal scanner based on CZT and assessing its performance potentials.

More accurate modelling of timing dependence due to electron drift time variations is under consideration. These models will take into account cathode signal shape dependence with depth of interaction.

REFERENCES

[1] D. Visvikis, T. Lefevre, G. Kontaxakis, and D. Darambara, "Monte Carlo based performance assessment of different animal PET scanner architectures using pixellated CZT detectors," presented at ITBS2005-3rd International Conference on Imaging Technologies in Biomedical Sciences, Milos, Greece, 2005.

[2] S. Jan, et al., "GATE: a simulation toolkit for PET and SPECT," *Physics in Medicine and Biolgy*, vol. 49, pp. 4543-4561, 2004.

[3] L.-A. Hamel and S. Paquet, "Charge transport and signal generation in CdTe pixel detectors," *Nuclear Instruments and Methods in Physics Research Section A*, vol. 380, pp. 238-240, 1996.

[4] A. Glière, M. Rosaz, and L. Verger, "Simulation of CdZnTe gamma-ray spectrometer response," *Nuclear Instruments & Methods In Physics Research Section A*, vol. 442, 2000.

[5] J. A. Heanue, J. K. Brown, and B. H. Hasegawa, "Two-dimensional modeling of Cd(Zn)Te strip detectors," *IEEE Transactions on Nuclear Science*, vol. 44, pp. 701 - 707, 1997.

[6] F. Mathy, et al., "A three-dimensional model of CdZnTe gamma-ray detector and its experimental validation," *IEEE Transactions on Nuclear Science*, vol. 51, pp. 2419-2426, 2004.

[7] M. Picone, A. Glière, and P. Massé, "A three-dimensional model of CdZnTe gamma-ray spectrometer," *Nuclear Instruments and Methods in Physics Research Section A*, vol. 504, pp. 313-316, 2003.

[8] S. Ramo, "Currents induced by electron motion," *Proceedings of the Institute of Radio Engineers*, pp. 584-585, 1939.

[9] Z. He, "Review of the Shockley–Ramo theorem and its application in semiconductor gamma-ray detectors," *Nuclear Instruments and Methods in Physics Research Section A*, vol. 463, pp. 250-267, 2001.

[10] E. G. d'Aillon, et al., "Simulation and experimental results on monolithic CdZnTe gamma-ray detectors," *IEEE Transactions on Nuclear Science*, vol. 52, pp. 3096-3102, 2005.

[11] A. Castoldi, E. Gatti, and P. Rehak, "Three-dimensional analytical solution of the Laplace equation suitable for semiconductor detector design," *IEEE Transactions on Nuclear Science*, vol. 43, pp. 256 - 265, 1996.

[12] W. Li, et al., "Experimental results from an Imarad 8x8 pixellated CZT detector," *Nuclear Instruments and Methods In Physics Research Section A*, vol. 458, pp. 518-526, 2001.

[13] R. Amrami, et al., "PET properties of pixellated CdZnTe detector," 2000.

[14] L. J. Meng and Z. He, "Exploring the limiting timing resolution for large volume CZT detectors with waveform analysis," *Nuclear Instruments & Methods In Physics Research Section A-Accelerators Spectrometers Detectors And Associated Equipment*, vol. 550, pp. 435-445, 2005.

[15] Y. Okada, et al., "CdTe and CdZnTe detectors for timing measurements," *IEEE Transactions on Nuclear Science*, vol. 49, pp. 1986, 2002.